Cellulose (2021) 28:11037–11049
https://doi.org/10.1007/s10570-021-04217-7

ORIGINAL RESEARCH

Preparation of cotton fibers modified with aromatic heterocyclic compounds and study of Cr(VI) adsorption performance

Zhiyu Huang · Peng Wu · Yankun Yin · Xiang Zhou · Lu Fu · Luoxin Wang · Shaohua Chen · Xu Tang

Received: 8 May 2021 / Accepted: 17 September 2021 / Published online: 26 September 2021

Abstract In order to prepare low-cost, biodegradable and processable adsorbent materials for adsorption of heavy metal ion, two kinds of novel modified cottons (C-4-APD and C-2-APZ) were obtained by introducing 4-aminopyridin and 2-aminopyrazine into the surface of degreasing cotton, respectively, and used for the removal of Cr(VI) ions from aqueous solution. The two modified cottons were characterized by Scanning Electron Microscopy (SEM), Fourier Transform Infrared Spectroscopy (FTIR) and X-ray photoelectron spectroscopy (XPS), which confirmed the amino groups, pyridine groups and pyrazine groups grafted onto the surface of modified cottons. The maximum adsorption capacities of C-4-APD and C-2-APZ were 89.66 mg/g and 54.92 mg/g, respectively, at the optimum pH of 2 and an initial concentration of 300 mg/g. Kinetic, isotherm and thermodynamic studies were carried out to investigate the adsorption behavior of the modified cottons on Cr(VI) ions. The results showed that the adsorption of Cr(VI) ions by modified cottons followed a pseudo-second-order kinetic model, the equilibrium data were in good agreement with the Langmuir isotherm model, and the thermodynamic analysis indicates that the adsorption proceeds spontaneously. The recovery and reuse of modified cotton were achieved by washing with 2 wt% thiourea-hydrochloric acid solution (0.5 mol/L concentration of HCl), and the adsorption capacities of C-4-APD and C-2-APZ were maintained above 90% and 85%, respectively, after six cycles.

Keywords Degreasing cotton · Chromium · Adsorption · Aminopyridine · Aminopyrazine · Surface modification

Introduction

The presence of chromium in the environment is generally Cr(III) and Cr(VI). Trace amounts of Cr(III) can reduce the blood glucose concentration in the human body to a certain extent, accelerate the metabolic process of sugar and substances required by the body, and the human insulin activity and stress response capacity can also be regulated by Cr(III) (Kooshki et al. 2021; Moradi et al. 2019). Cr(VI) has

Zhiyu Huang and Peng Wu as co-first author contributed equally to this work.

Z. Huang · Y. Yin · X. Zhou · L. Fu · L. Wang · S. Chen (✉)
Key Laboratory of Textile Fibers and Products, P. R. C, College of Materials Science and Engineering, Ministry of Education, Wuhan Textile University, Wuhan 430200, China
e-mail: shaohuachen@foxmail.com

P. Wu · X. Tang (✉)
Third Institute of Oceanography Ministry of Natural Resources, P. R. C, Xiamen 361005, China
e-mail: tangxu@tio.org.cn

higher mobility, bioavailability and carcinogenic effect, and is 100 times more toxic than Cr(III), which can cause more serious harm to various organisms (Kimbrough et al. 1999; Singh and Chowdhuri 2017). At present, the main methods for treating chromium-containing wastewater are adsorption (Sun et al. 2021), chemical (Bao et al. 2020), ion exchange (Li et al. 2017), electrochemical (Yao et al. 2020) and biological methods (Long et al. 2020), etc. The most industrial application is adsorption method, which is suitable for the deep purification of low concentration chromium-containing wastewater because of its simplicity and convenience (Zhao et al. 2015). However, most of the adsorbents reported in the literature for the removal of hexavalent chromium are prepared under complicated process conditions, raw materials are not easily available, costs are high, and they are also difficult to degrade in the natural environment, which may cause se condary pollution to the environment in practical applications.

Biomass materials are widely available, relatively low-priced, with large specific surface area, good stability and biodegradable, etc. At the same time, the surface of biomass materials is rich in hydroxyl groups and other reactive groups, which can be regulated and functionalized by chemical or physical methods, and are ideal choices for carrier materials (Xu et al. 2016), such as cellulose (Park et al. 2020; Sharma et al. 2018), lignin(Wu et al. 2008), hemicellulose (Wei et al. 2021), chitosan (Vakili et al. 2018; Eliodorio et al. 2017), etc. Highly efficient adsorbents were prepared by grafting the cellulose with functional groups (Zhang et al. 2019; Xie et al. 2017; Li et al. 2018), Liang et al. (2020) reported the maximum Cr(VI) uptake was 490.3 mg/g for quaternized cellulose grafted with polyethyleneimine in the presence of epichlorohydrin. The imidazole groups were successfully grafted onto the macroporous cellulose by a homogeneous method to fabricate 3D macroporous materials with synergistic advantages of cellulose and polyvinylimidazole, and the optimized adsorbent exhibited a fast adsorption rate (0.12 g/(mg/min)) and high adsorption capacity (134 mg/g)(Peng et al. 2020). However, for crude processed biomass materials such as cotton, hemp, and agricultural wastes, the corresponding reports are less available and have a low Cr(VI) adsorption capacity. For example, Rojas et al. (2018) reported the removal of Cr(VI) from water using cotton fibers coated with deacetylated chitosan, and the adsorption capacity for Cr(VI) was 7.5 mg/g at pH 2.0. The crude processed biomass material is more widely available and if it is utilized to improve and increase its adsorption capacity for Cr(VI), the processing steps for preparing biomass-based adsorbents can be more simplified and less costly.

Pyridines and pyrazines are important intermediate compounds that are widely used in the synthesis of medical (agricultural) drugs and in the preparation of dyes, and they can also be used as drugs and analytical reagents themselves. However, there are few reports on the use of pyridines and pyrazines for contaminant treatment. By electron-donating nitrogen, as well as electron-rich π-conjugated structures, and the nitrogen atoms in pyridine group and pyrazine group form hydrogen bonds, so the polymer containing pyridine group or pyrazine group has the ability of coordination chelation, which can be used for the removal of metal ions in solution and environmental pollution control. Geng et al. (2020) reported that two kinds of fluorescent conjugated microporous polymers containing pyrazine moieties were prepared by the polymerization reaction of 2,5-di-triphenylamine-yl-pyrazine(DTPAPz) and N,N,N',N'-tetrapheny-2,5-(-diazyl) pyrazine (TDPz), for adsorbing and fluorescent sensing of iodine. Bayramoglu et al. (2016) reported that aminopyridine modified Spirulina platensis biomass for Cr(VI) adsorption in aqueous solution. chemical modification of Spirulina platensis biomass was realized by sequential treatment of algal surface with epichlorohydrin and aminopyridine. The adsorption capacity at pH 3.0 was found to be 79.6 and 158.7 mg/g, for native and modified algal biomasses, respectively. Zheng et al. (2019) and Bayramoglu and Arica (2011) synthesized particles with high specific surface area and high adsorption capacity of 344.83 mg/g and 172.11 mg/g, respectively, for Cr(VI) using vinyl pyridine. It is clear from these studies that pyridines and pyrazines have good potential for the treatment of heavy metal ions and other contaminants.

Therefore, in order to prepare low-cost, biodegradable and processable adsorbent materials, 4-aminopyridine and 2-aminopyrazine were introduced to the surface of degreasing cotton using one-pot method in this study. The cotton-4-aminopyridine(C-4-APD) and the cotton-2-aminopyrazine(C-2-APZ) were obtained and used for the removal of Cr(VI) ions

from aqueous medium. The morphology and structure property of the prepared samples were characterized by the SEM, FTIR, XPS and BET. Additionally, the adsorption behavior and thermodynamic of Cr(VI) on C-4-APD and C-2-APZ was investigated by Langmuir and Freundlich models, and the experimental data were fitted by two kinetic models, pseudo-first-order and pseudo-second-order(Simonin 2016), to analyze the mechanism of Cr(VI) adsorption, and its reusability was evaluated by repeated adsorption-elution, and the effect of ionic strength was also compared.

Experiment

Materials

Potassium chromate(99.9% metals basis), 4-aminopyridin(98%) and 2-aminopyrazine(99%) were purchased from Shanghai Macklin Biochemical Co., Ltd(Shanghai, China). Epichlorohydrin, N,N-dimethylformamide (DMF), hydrochloric acid(30%) and thiourea(AR 99%) were purchased from Sinopharm Chemical Reagent Corp (Shanghai, China). Degreasing cotton was supplied from Xuzhou Weicai Hygiene of Material Factory Co. LTD (Xuzhou, China).

Preparation of cotton-4-aminopyridin and cotton-2-aminopyrazine

1 g of degreasing cotton was soaked in the solvent of 50 mL of N,N-dimethylformamide and 50 mL of epichlorohydrin to soak. In the first stage, the reaction temperature was controlled at 80 °C, and the chloromethylated cotton was stirred slowly for 2 h with a magnetic stirrer to obtain chloromethylated degreasing cotton; In the second stage, 10 mmol of 4-aminopyridin or 2-aminopyrazine was accurately added to the above solution. The mixture continued to be stirred for 5 h at 90 °C. The mass ratio of reactants to products, degreasing cotton: epichlorohydrin: 4-aminopyridine: 2-aminopyrazine: C-4-APD: C-2-APZ = 1: 59: 0.941: 0.951: 1.35 ± 0.05: 1.4 ± 0.05. The procedure for preparation of C-4-APD/C-2-APZ is illustrated in Fig. 1.

Characterization

Surface morphological characteristics of degreasing cotton, C-4-APD and C-2-APZ were examined by scanning electron microscopy (SEM) using a JSM-IT300A scanning electron microscope(JEOL Ltd.,Tokyo, Japan). Bonding structure and surface functionalization of samples were conducted on a VERTEX 70 FT-IR spectrometer by using potassium bromide pressed-disk technique, respectively. The scan range was 400 to 4000 cm^{-1}. The elemental composition of the samples was measured by XPS using Thermo Scientific K-Alpha (Thermo Fisher). The pore condition of the samples was measured by BET using ASAP 2460 Version 2.02 (Micromeritics).

Adsorption experiments

The effect of pH of the reaction system on the Cr(VI) adsorption capacity brought by C-4-APD and C-2APZ in Cr(VI) adsorption experiments, as well as their adsorption thermodynamics, adsorption kinetics, and recyclability were investigated by a series of adsorption experiments. All Cr(VI) adsorption experiments were performed in 150 mL beakers and shaken at 120 rpm in a mechanical shaker. To explore the effect of pH on the Cr(VI) adsorption capacity, 0.1 g of C-4-APD/C-2-APZ was placed into 100 ml of 100 mg/L Cr(VI) solution with different pH values. The pH was adjusted by concentrations of 0.5 M and 1 M hydrochloric acid. Cr(VI) concentrations were determined by ICP 2060 T inductively coupled plasma emission spectrometer (Jiangsu Tianrui Instruments Co., Ltd., Kunshan, China), and the adsorption capacity of modified cotton for Cr(VI) was calculated as follows:

$$Q = \frac{(C_0 - C_e) \times V}{m} \quad (1)$$

where C_0 and C_e (mg/L) are the initial concentration and the equilibrium concentration of Cr(VI), V (L) is the volume of Cr(VI) solution, and m (mg) is the mass of the modified cotton.

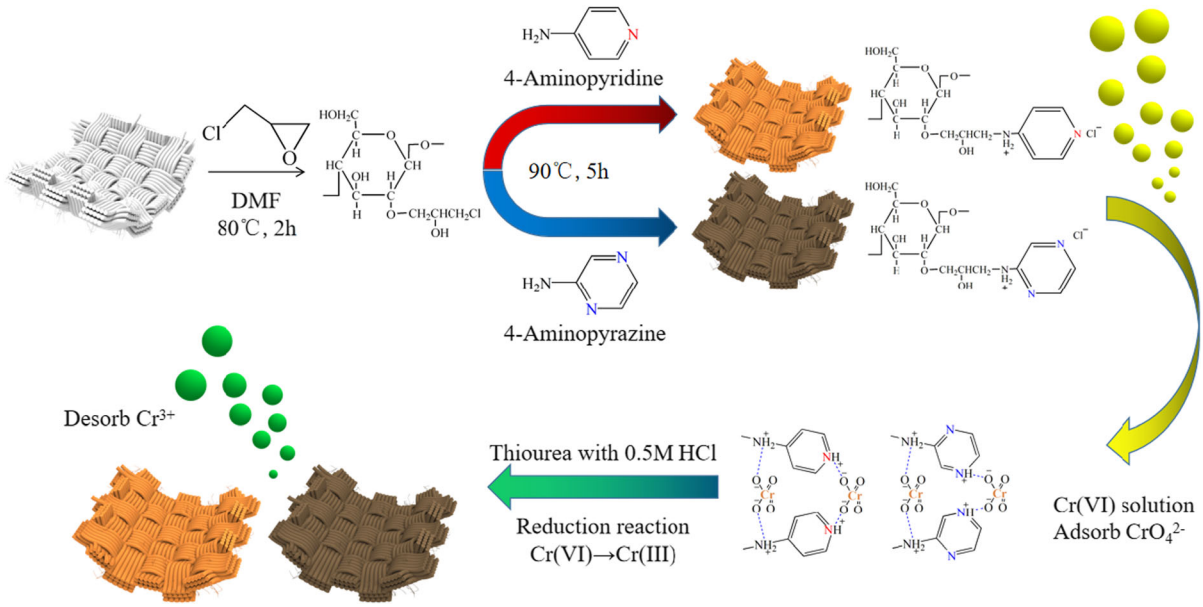

Fig. 1 Schematic illustration of the C-4-APD and C-2-APZ preparation process

Results and discussion

Characterization of the samples

Figure 2 shows the scanning electron micrographs of degreasing cotton, C-4-APD and C-2-APZ. The surface of the degeasing cotton fiber was smooth and the diameter of the cotton fiber was about 15 um as seen in Fig. 2a. From Fig. 2b and Fig. 2c, it was observed that the surfaces of both C-4-APD and C-2-APZ become rough, indicating that organic monomers are grafted on the surface of cotton fibers.

Figure 3 shows the FTIR spectra of degreasing cotton, C-4-APD and C-2-APZ. The FTIR profiles of degreasing cotton: the peaks at 3315 cm^{-1} are caused by stretching vibrations due to the presence of a large number of hydroxyl hydrogen bonds in the cotton fiber; the peaks at 1407 cm^{-1} and 1303 cm^{-1} are caused by the bending vibrations of CH_2 and CH present in large quantities in the cellulose backbone structure, respectively; the characteristic absorption bands at 1149 cm^{-1} and 1019 cm^{-1} are each The characteristic absorption bands at 1149 cm^{-1} and 1019 cm^{-1} are each attributed to the asymmetric stretching vibration of C–O–C and the stretching vibration of C-O in the cellulose six-membered ring structure(Wang et al. 2019). After attachment of 4-aminopyridine/2-aminopyrazine via epichlorohydrin coupling reaction, the spectrum of the modified degreasing cotton exhibits some changes. The peak formed at 3244 cm^{-1} was an N–H stretching vibration peak in the imine group (Bayramoglu et al. 2016).

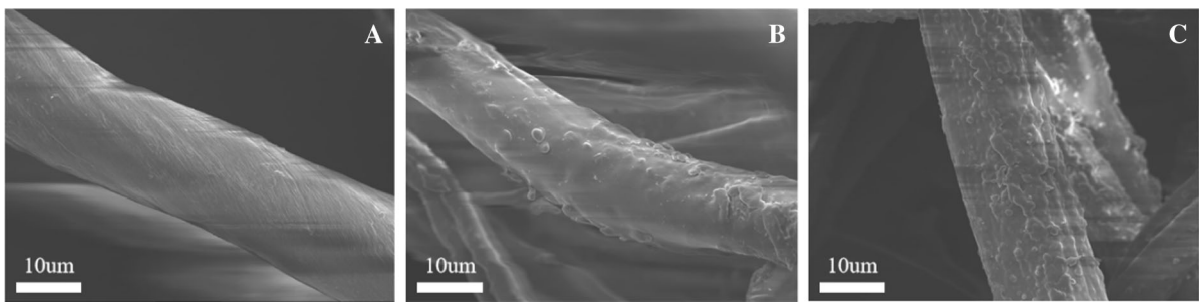

Fig. 2 SEM images of the degreasing cotton **a**, C-4-APD **b** and C-2-APZ **c**

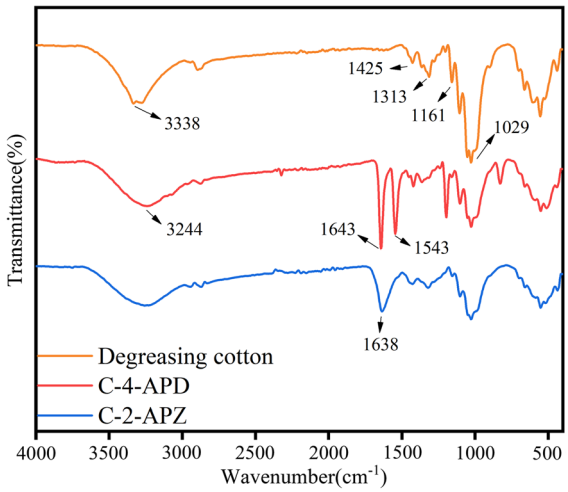

Fig. 3 FTIR spectra of degreasing cotton, C-4-APD and C-2-APZ

Besides, the new characteristic peaks observed at 1643 cm^{-1}, 1638 cm^{-1}, and 1543 cm^{-1} are caused by C = N and C-N bonds in the aromatic heterocycles, confirming the successful grafting of pyridine and pyrazine groups on the degreasing cotton surface(Hu et al. 2014; Lu et al. 2020).

The mass fraction of elements of the degreasing cotton, C-4-APD and C-2-APZ were determined using XPS to study the amount of aromatic heterocyclic compounds introduced. As shown in Table 1, the degreasing cotton contains almost no elemental N. After grafting the 4-aminopyridine and 2-aminopyrazine onto the surface of the degreasing cotton, the N elemental content of C-4-APD and C-2-APZ increased significantly, which further proved the successful introduction of 4-aminopyridine and 2-aminopyrazine on the surface of degreasing cotton.

The pore condition of the samples was measured by BET. As shown in Table 2, There was no significant change in total area, indicating that the modified cotton did not increase the adsorption capacity by increasing the specific surface area.

Table 1 The mass fraction of elements of degreasing cotton, C-4-APD and C-2-APZ

Materials	C/%	N/%	O/%
Dgreasing cotton	70.83	0.59	28.58
C-4-Aminopyridine	69.7	5.52	24.78
C-2-Aminopyrazine	65.28	9.69	25.03

Batch adsorption studies

Effect of pH

Figure 4 shows the difference in the adsorption capacity of C-4-APD and C-2-APZ for Cr(VI) in the range of solution pH from 2 to 8, with an adsorption time of 4 h. In aqueous media, Cr(VI) ions exist mainly as soluble oxides, and the ionic species depend on the pH of the medium and the total concentration of Cr(VI) in the solution, when the solution pH is less than 2.0, the dominant species is H_2CrO_4. When the solution pH is greater than 6.4, only CrO_4^{2-} is present, while the solution pH is between 2.0 and 6.4, $HCrO^{4-}$ and $Cr_2O_7^{2-}$ dominate (Bayramoglu et al. 2016; Zheng et al. 2019). It can be seen from graphs that the adsorption of Cr(VI) by C-4-APD and C-2-APZ increases as the pH decreases, which mainly due to the N atoms in the pyridine, pyrazine and imine groups are prone to binding H + under acidic conditions leading to protonation and gravitational binding between them and the negatively charged Cr(VI) anion, resulting in an increase in the removal efficiency of Cr(VI). As shown in Fig. 4, both adsorbents were highly dependent on the pH of the medium, and the adsorption capacity of the former was higher than that of the latter, which was due to the different electron cloud distribution of the N atoms between the 4-aminopyridin and 2-aminopyrazine. The N atoms of the pyridine group in 4-aminopyridin are in the opposite position of the amino group, which have stronger ability to bind H^+ when protonated, while the N atoms of pyrazine group in 2-aminopyrazine are in the adjacent and interposition of amino group, respectively, of which the electron cloud distribution was more dispersed, and the ability of binding H^+ was weaker when protonated. At the solution pH less than 2.0, the degreasing cotton skeleton started to be decomposed by corrosion, thus, it was determined that the adsorption capacity of C-4-APD and C-2-APZ for Cr(VI) reached the maximum at pH = 2.0, and the subsequent experiments were carried out at this pH value.

Table 2 The pore of degreasing cotton, C-4-APD and C-2-APZ

Materials	Average pore diameter/nm	Total volume in pores/(cm^3 g^{-1})	Total area in pores/(m^2 g^{-1})
Degreasing cotton	1.269	0.06607	22.132
C-4-APD	2.114	0.07268	25.95
C-2-APZ	2.19	0.08112	26.035

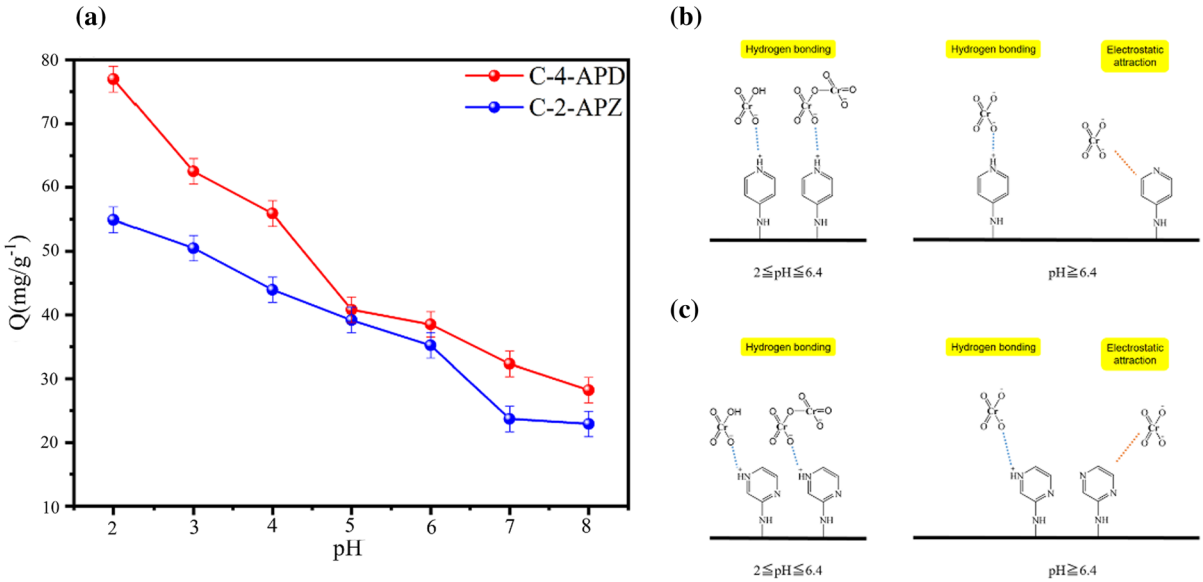

Fig. 4 Effect of the pH value on the adsorption of Cr (VI) ions by C-4-APD and C-2-APZ

Adsorption kinetics

Figure 5A shows the effect of adsorption time on the Cr(VI) ions adsorption capacity of C-4-APD and C-2-APZ. The adsorption rate of Cr(VI) was high within 30 min and approached the saturation level at about 360 min.

In order to investigate a range of kinetic factors for the adsorption of Cr(VI) ions by C-4-APD and C-2-APZ, pseudo-first-order and pseudo-second-order kinetic models were used to fit the kinetic data:

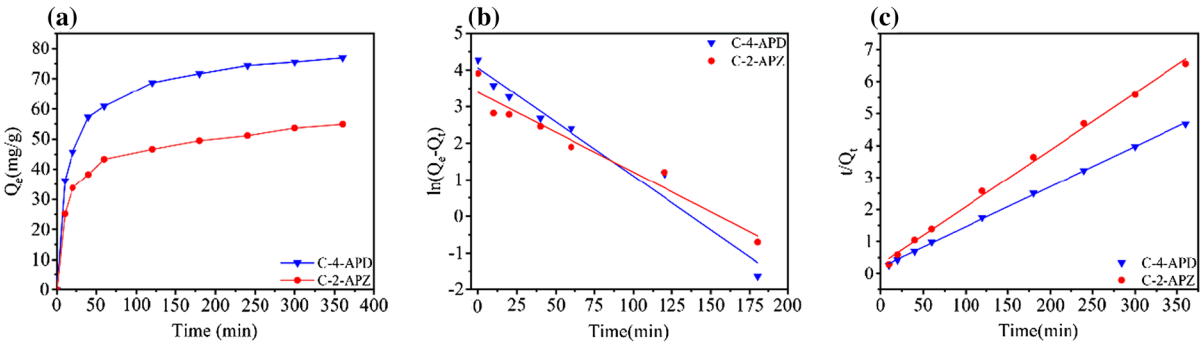

Fig. 5 Effect of contact time on the Cr(VI) ions adsorption capacity of C-4-APD and C-2-APZ **a**; The curve fitting with pseudo-first-order **b** and pseudo-second-order kinetics model **c**

$$\ln(Q_e - Q_t) = \ln Q_e - k_1 t \quad (2)$$

$$\frac{t}{Q_t} = \frac{1}{k_2 Q_e^2} + \frac{1}{Q_e} t \quad (3)$$

where Q_e (mg/g) and Q_t (mg/g) are the adsorption capacities of Cr(VI) ions at equilibrium and time t (min) respectively; k_1 (min^{-1}) and k_2 ((g/mg)/min) are the pseudo-first-order rate constant and pseudo-second-order rate constant, respectively.

Figure 5b and c are the fitted curves of the pseudo-first-order and pseudo-second-order kinetic models for the actual experimental data of C-4-APD and C-2-APZ, and a series of kinetic parameters calculated and fitted by the two adsorption equations are shown in Table 3. As can be seen from the table, the correlation coefficient R^2 of the fitted curves of the pseudo-first-order model was higher than that of the fitted curves of the pseudo-second-order model, which were closer to 1. And the theoretical Q_e values of the adsorbent in the case of pseudo-second-order kinetics are very close to the experimental Q_e values, it was considered that C-4-APD and C-2-APZ for Cr(VI) ions follow the pseudo-second-order model, and This suggests that the rate-limiting step may be the chemical adsorption not the mass transport limitation(Bayramoglu and Yakuparica 2008; Bayramoglu et al. 2007).

Adsorption isotherm and thermodynamic analysis

Figure 6a and d shows the adsorption isotherms of Cr(VI) ions by C-4-APD and C-2-APZ. It can be seen from the figure that the adsorption capacities of C-4-APD and C-2-APZ for Cr(VI) ions were almost the same at the initial concentration of Cr(VI) ions below 50 mg/L. However, as the initial concentration continued to increase, C-4-APD showed better adsorption behavior, which also indicated that C-4-APD had better proton binding ability. When the concentration of Cr(VI) ions solution increased to about 300 mg/L, the adsorption capacities of C-4-APD and C-2-APZ for Cr(VI) ions basically ceased to change at room temperature. The highest adsorption capacities of C-4-APD and C-2-APZ for Cr(VI) ions were about 89.66 mg/g and 54.92 mg/g, respectively. By comparing with the maximum adsorption capacities of other surface modified biomass materials (Table 4), we can find that the adsorption capacities of C-4-APD and C-2-APZ were better, moreover, C-4-APD and C-2-APZ are very easy to separate from solution, compared to high specific surface area of particulate or nanoparticle materials.

The Langmuir model predicts the formation of an adsorbed solute monolayer, with no side interactions between the adsorbed ions, which also assumes that the interactions take place by adsorption of one ion per binding sites and that the adsorbent surface is homogeneous and contains only one type of binding site, and the Freundlich model does not predict surface saturation, which considers the existence of a multilayered structure(Bayramoglu et al. 2007; Bayramoglu and Yakuparica 2008). Langmuir and Freundlich models were frequently used to evaluate the saturation binding data, the two equations are expressed as follows:

$$\frac{C_e}{Q_e} = \frac{1}{k_L Q_{max}} + \frac{C_e}{Q_{max}} \quad (4)$$

$$\ln\ Q_e = \ln\ k_F + \frac{1}{n} \ln C_e \quad (5)$$

where Q_e (mg/g) is the amount of Cr(VI) ions bound to the C-4-APD and C-2-APZ at equilibrium, C_e (mg/L) is the equilibrium concentration, and Q_{max} (mg/g) is the apparent maximum adsorption capacity. K_L is the Langmuir constant, K_F and 1/n are the Freundlich constants.

The fits of Langmuir and Freundlich isothermal adsorption models for Cr(VI) ions adsorbed by C-4-APD and C-2-APZ were shown in Fig. 6(b-f). The

Table 3 Kinetic parameters for Cr(VI) ions uptake by C-4-APD and C-2-APZ

Sample		Pseudo-first-order			Pseudo-second-order		
	Q_m(mg/g)	Q_e(mg/g)	k_1(min^{-1})	R^2	Q_e(mg/g)	k_2((g/mg)/min)	R^2
C-4-APD	76.99	71.893	0.05003	0.957	77.794	0.000953	0.995
C-4-APZ	54.91	49.98	0.0519	0.944	54.162	0.0014	0.989

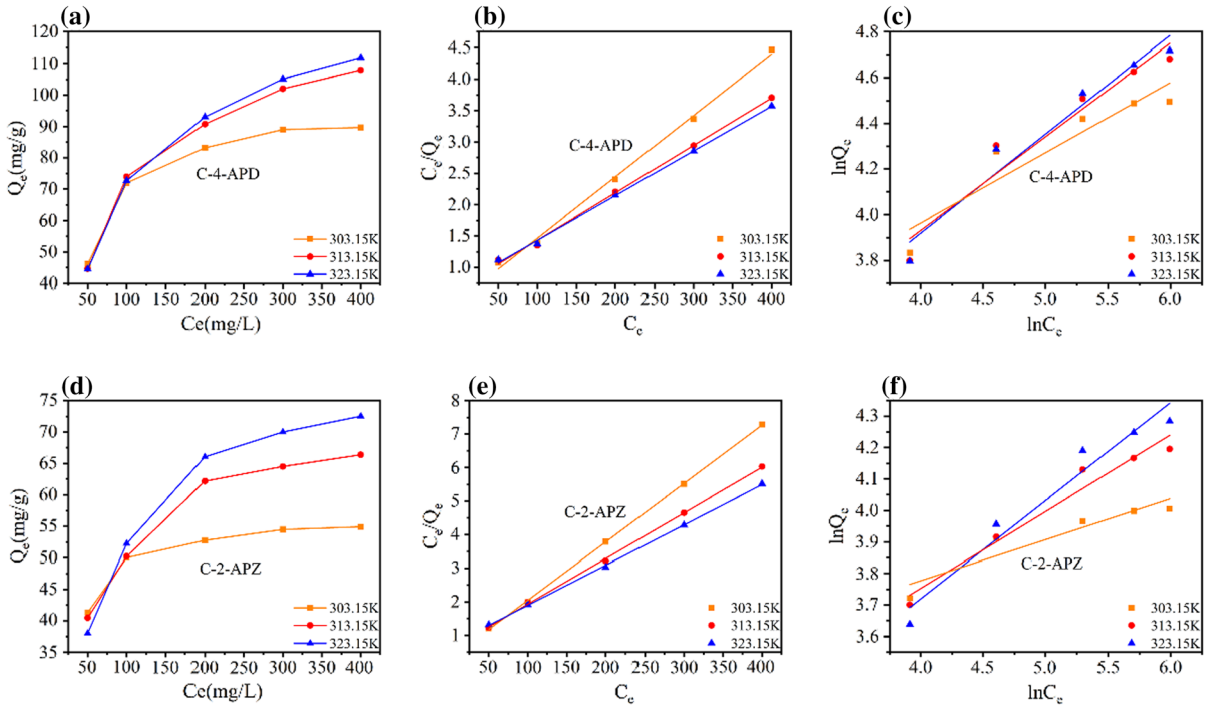

Fig. 6 Adsorption isotherms for Cr(VI) adsorption on C-4-APD **a** and C-2-APZ **d** at 303.15, 313.15, and 323.15 K; The curve fitting with the Langmuir **b, e** and Freundlich model **c, f**

Table 4 Comparison of adsorption capacities for Cr(VI) ions on various surface modified biomass materials

Adsorbents	Adsorption capacity (mg/g)	Reference
Activated Carbon	22.29	(Mohan et al. 2005)
Modified zeolite	29.7	(Ghiaci et al. 2004)
Pine / TiO2	12.8	(Zhao et al. 2021)
PEI-cellulose composite	36.8	(Qiu et al. 2014)
Cotton Fiber/ZrO2	69.13	(Muxel et al. 2011)
cotton stalks biochar	54.95	(Tariq et al. 2020)
cotton stalks biochar/ ZnO nanoparticles	107.53	(Tariq et al. 2020)
Ficus auriculata leaves	13.3	(Rangabhashiyam et al. 2014)
cotton/chitosan	7.5	(Rojas et al. 2018)
Immobilized corn cob	112.49	(Manzoor et al. 2019)
C-4-APD	89.66	this work
C-2-APZ	54.92	this work

isotherm parameters of the two models were listed in Table 5. From the fitted curves, it can be seen that the correlation coefficients R^2 of the linear equations after fitting the Langmuir equation were closer to 1 than those of the Freundlich model, which proves that the Langmuir model can describe the experimental measured data more closely. In addition, the maximum adsorption capacities of C-4-APD and C-2-APZ were different from the experimental adsorption capacity. This was due to the formation of hydrogen bonds between the groups in C-4-APD or C-2-APZ, which occupy the adsorption sites and make the actual

Table 5 Parameters for Cr(VI) ions adsorption by C-4-APD and C-2-APZ according to different equilibrium models

C-4-APD	Q_e(mg/g)	Langmuir			Freundlich		
		Q_m(mg/g)	k_L(L/mg)	R^2	1/n	k_F(L/g)	R^2
303.15 K	89.66	104.6	0.0183	0.971	0.269	18.881	0.881
313.15 K	107.92	132.1	0.0113	0.991	0.365	12.609	0.948
323.15 K	111.9	140.252	0.00999	0.996	0.389	11.291	0.962
C-4-APZ	Q_e(mg/g)	Langmuir			Freundlich		
		Q_m(mg/g)	k_L(L/mg)	R^2	1/n	k_F(L/g)	R^2
303.15 K	54.92	57.971	0.0528	0.981	0.124	26.89	0.883
313.15 K	66.37	73.8	0.0234	0.991	0.231	17.189	0.953
323.15 K	72.55	84.175	0.0167	0.997	288	13.454	0.951

maximum adsorption capacity lower than the calculated value. Furthermore, the large size of $Cr_2O_7^{2-}$ makes it difficult to enter the adsorption sites, thus limiting the adsorption capacity of $Cr_2O_7^{2-}$(Fenti et al. 2020). These indicated a homogeny adsorption process, leading to monolayer binding.

The experimental data obtained at different temperatures were used to calculate the thermodynamic parameters of Cr(VI) on modified cotton. The thermodynamic parameters, namely, the Gibbs free energy change (ΔG), standard enthalpy change (ΔH), and standard entropy change (ΔS), were calculated according to the following equations to evaluate the adsorption thermodynamic behavior(Zheng et al. 2019; Shi et al. 2020):

$$\ln K_d = \frac{\Delta H}{RT} + \frac{\Delta S}{R} \quad (6)$$

$$\Delta G = \Delta H - T\Delta S \quad (7)$$

where K_d (mL/g) is the thermodynamic equilibrium constant; and ΔH (KJ/mol) and ΔS (kJ/mol/K) can be determined from the slope and intercept of the linear plot of ln K_d versus 1/T, respectively(Shi et al. 2020).

As illustrated in Table 6, the negative ΔG and positive ΔH values implied spontaneous and endothermic nature, respectively. The positive ΔS value manifested the increased disorder and randomness at the solid–liquid interface during the adsorption of Cr(VI) on the surface of modified cottons(Song et al. 2016).

Effect of ionic strength

Dissolved salt ions can interfere with Cr(VI) adsorption by ion exchange, therefore, the effect of ionic strength on Cr(VI) removal by C-4-APD and C-2-APZ was investigated as shown in Fig. 7. In this experiment, the concentration of Cr(VI) was 400 ppm. As the concentration of NaCl or $NaSO_4$ increased from 0 M to 0.1 M, the inhibition of Cr(VI) removal by coexisting salt ions (NaCl or $NaSO_4$) was not significant, and the adsorption capacities remained above 80% and 88%, respectively. Therefore, the main mechanism of Cr(VI) removal by modified cotton is not ion exchange.

Reusability studies

Desorption and regeneration of adsorbent is one of the most important properties of adsorption separation technology. a thiourea-hydrochloric acid solution with a mass fraction of 2 wt% (the concentration of HCl was 0.5 mol/L) was chosen as the eluent. The mixed thiourea-hydrochloric acid solution can not only elute the Cr(VI) ions from the binding sites, but also thiourea can reduce Cr(VI) to the less toxic Cr(III) under acidic conditions. To investigate the reusability and stability of C-4-APD and C-2-APZ, we performed six adsorption–desorption processes using the same C-4-APD and C-2-APZ, and the adsorption amounts of the six experiments were in Fig. 8. As can be seen from the figure, the adsorption capacities of C-4-APD and C-2-APZ for Cr(VI) ions with multiple reuses did not change evidently and remained above 90 and 85%, which proved that C-4-APD and C-2-APZ have good

Table 6 Thermodynamic parameters for Cr(VI) adsorption onto C-4-APD and C-2-APZ

C-4-APD	T (K)	ΔG (kJ/mol)	ΔH (kJ/mol)	ΔS (kJ/mol/K)
	303.15	−5.966	22.864	0.0951
	313.15	−6.917		
	323.15	−7.868		
C-4-APZ	T (K)	ΔG (kJ/mol)	ΔH (kJ/mol)	ΔS (kJ/mol/K)
	303.15	−3.453	43.535	0.155
	313.15	−5.003		
	323.15	−6.553		

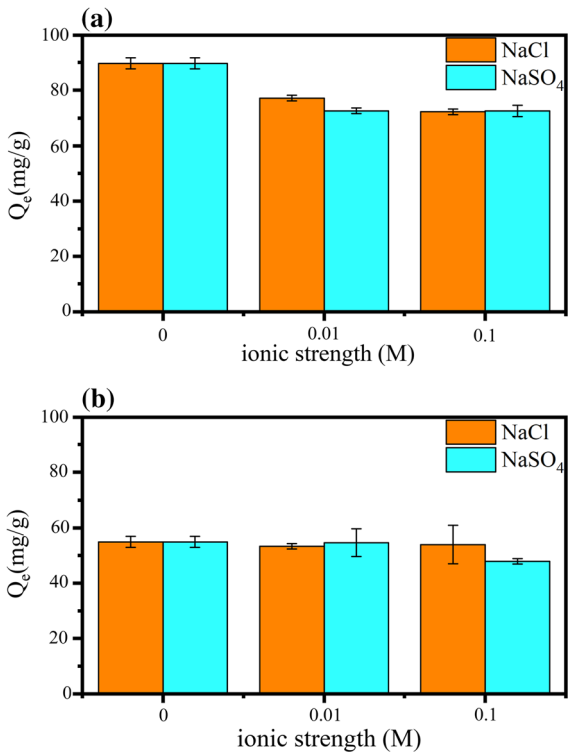

Fig. 7 Effect of ionic strength on Cr(VI) removal by C-4-APD **a** and C-2-APZ **b**. (Cr(VI) conc. = 300 mg/L; pH = 2; temp. = 303.15 K)

reusability and stability. Which was due to the excellent flexibility of degreasing cotton as a substrate, the adsorption sites were not easily destroyed and deformed. Furthermore, the adsorption sites encapsulated by hydrogen bonds can replace the destroyed adsorption sites to some extent after multiple washes. Thus, the multiple adsorption–desorption process has less effect on the adsorption capacity of C-4-APD and C-2-APZ.

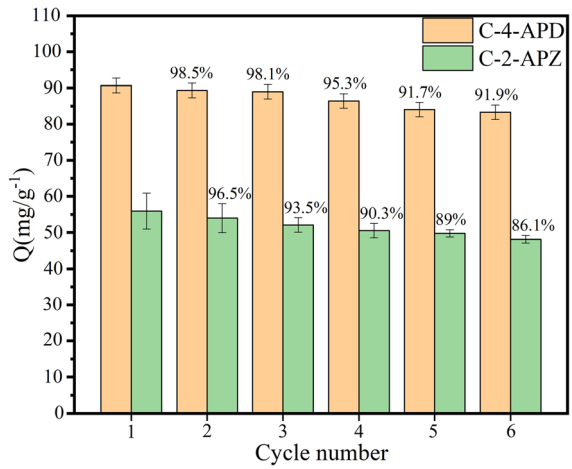

Fig. 8 Regeneration of C-4-APD and C-2-APZ. (Cr(VI) conc. = 300 mg/L; pH = 2; temp. = 303.15 K)

Conclusions

In summary, 4-aminopyridine and 2-aminopyrazine were successfully introduced to the surface of cotton fiber and used to remove Cr(VI) ions from aqueous solution in this study. SEM, FT-IR and XPS that a large number of amino, pyridine and pyrazine groups were introduced to the surface of cotton fiber after modification by 4-aminopyridine and 2-aminopyrazine. The Cr(VI) ions on the modified cotton fiber adsorption was mainly achieved by electrostatic interactions between the protonated functional groups on the adsorbent and the Cr(VI) anions. The maximum adsorption capacities of C-4-APD and C-2-APZ were 89.66 mg/g and 54.92 mg/g, respectively, at the optimum pH of 2 and an initial concentration of 300 mg/g. Kinetic studies showed that the adsorption process followed the pseudo-second-order kinetic model indicating that chemisorption as a rate-limiting

step that controls the adsorption process. The adsorption isotherm analysis showed that the Langmuir model was in good agreement with the adsorption equilibrium data and the adsorption was the monolayer adsorption process. The thermodynamic analysis indicates that the adsorption proceeds spontaneously. In addition, the adsorption capacities of adsorbents didn't significantly decrease after dissolving other salt ions or six times of repeated use. These results indicate the potential application of 4-aminopyridine and 2-aminopyrazine modified cotton fibers in the removal of Cr(VI) ions from aqueous solutions.

Acknowledgments The authors appreciate the financial support from The Natural Science Foundation of Fujian Province of China (2020J01103).

Author contributions Conceptualization: ZYH, PW, SHC, XT; Methodology: ZYH; Investigation: ZYH, PW; Formal analysis: ZYH, PW; Writing—original draft preparation: ZYH; Writing—review and editing: ZYH, PW, XZ, YKY, LF, SHC, XT; Funding acquisition: SHC, XT, LXW; Resources: SHC, XT, LXW; Supervision: ZYH, PW, SHC, XT.

Funding The Natural Science Foundation of Fujian Province of China (2020J01103).

Declarations

Conflict of interest The authors declare that they have no conflicts of interest to declare.

Ethical approval This article does not contain any studies with human participants or animals performed by any of theauthors.

References

Bao S, Liu H, Liu Y, Yang W, Wang Y, Yu Y, Sun Y, Li K (2020) Amino-functionalized graphene oxide-supported networked Pd-Ag nanowires as highly efficient catalyst for reducing Cr(VI) in industrial effluent by formic acid. Chemosphere 257:127245. https://doi.org/10.1016/j.chemosphere.2020.127245

Bayramoglu G, Akbulut A, Arica MY (2016) Aminopyridine modified Spirulina platensis biomass for chromium(VI) adsorption in aqueous solution. Water Sci Technol 74:914–926. https://doi.org/10.2166/wst.2016.281

Bayramoglu G, Arica MY (2011) Synthesis of Cr(VI)-imprinted poly(4-vinyl pyridine-co-hydroxyethyl methacrylate) particles: its adsorption propensity to Cr(VI). J Hazard Mater 187:213–221. https://doi.org/10.1016/j.jhazmat.2011.01.022

Bayramoglu G, Yakup Arica M, Bektas S (2007) Removal of Cd(II), Hg(II), and Pb(II) ions from aqueous solution using p(HEMA/chitosan) membranes. J Appl Polym Sci 106:169–177. https://doi.org/10.1002/app.26704

Bayramoglu G, Yakuparica M (2008) Adsorption of Cr(VI) onto PEI immobilized acrylate-based magnetic beads: Isotherms, kinetics and thermodynamics study. Chem Eng J 139:20–28. https://doi.org/10.1016/j.cej.2007.07.068

Eliodorio KP, Andolfatto VS, Martins MRG, De Sá BP, Umeki ER, De Araújo M-G (2017) Treatment of chromium effluent by adsorption on chitosan activated with ionic liquids. Cellulose 24:2559–2570. https://doi.org/10.1007/s10570-017-1264-3

Fenti A, Chianese S, Iovino P, Musmarra D, Salvestrini S (2020) Cr(VI) sorption from aqueous solution: a review. Appl Sci 10:6477. https://doi.org/10.3390/app10186477

Geng T, Ma L, Chen G, Zhang C, Zhang W, Niu Q (2020) Fluorescent conjugated microporous polymers containing pyrazine moieties for adsorbing and fluorescent sensing of iodine. Environ Sci Pollut Res Int 27:20235–20245. https://doi.org/10.1007/s11356-019-06534-8

Ghiaci M, Kia R, Abbaspur A, Seyedeyn-Azad F (2004) Adsorption of chromate by surfactant-modified zeolites and MCM-41 molecular sieve. Sep Purif Technol 40:285–295. https://doi.org/10.1016/j.seppur.2004.03.009

Hu Y, Zhang J, Yu C, Li Q, Dong F, Wang G, Guo Z (2014) Synthesis, characterization, and antioxidant properties of novel inulin derivatives with amino-pyridine group. Int J Biol Macromol 70:44–49. https://doi.org/10.1016/j.ijbiomac.2014.06.024

Kimbrough DE, Cohen Y, Winer AM, Creelman L, Mabuni C (1999) A critical assessment of chromium in the environment. Crit Rev Environ Sci Technol 29:1–46. https://doi.org/10.1080/10643389991259164

Kooshki F, Tutunchi H, Vajdi M, Karimi A, Niazkar HR, Shoorei H, Pourghassem Gargari B (2021) A Comprehensive insight into the effect of chromium supplementation on oxidative stress indices in diabetes mellitus: a systematic review. Clin Exp Pharmacol Physiol 48:291–309. https://doi.org/10.1111/1440-1681.13462

Li LL, Feng XQ, Han RP, Zang SQ, Yang G (2017) Cr(VI) removal via anion exchange on a silver-triazolate MOF. J Hazard Mater 321:622–628. https://doi.org/10.1016/j.jhazmat.2016.09.029

Li Y, Zhu H, Zhang C, Cheng M, He H (2018) PEI-grafted magnetic cellulose for Cr(VI) removal from aqueous solution. Cellulose 25:4757–4769. https://doi.org/10.1007/s10570-018-1868-2

Liang X, Liang B, Wei J, Zhong S, Zhang R, Yin Y, Zhang Y, Hu H, Huang Z (2020) A cellulose-based adsorbent with pendant groups of quaternary ammonium and amino for enhanced capture of aqueous Cr(VI). Int J Biol Macromol 148:802–810. https://doi.org/10.1016/j.ijbiomac.2020.01.184

Long B, Ye J, Ye Z, He J, Luo Y, Zhao Y, Shi J (2020) Cr(VI) removal by Penicillium oxalicum SL2: reduction with acidic metabolites and form transformation in the mycelium. Chemosphere 253:126731. https://doi.org/10.1016/j.chemosphere.2020.126731

Lu H, Wu F, Yang Y, Li S, Hua Y, Zhu L (2020) Hole transport materials based on a twisted molecular structure with a single aromatic heterocyclic core to boost the performance

of conventional perovskite solar cells. J Mater Chem C 8:13415–13421. https://doi.org/10.1039/d0tc03404e

Manzoor Q, Sajid A, Hussain T, Iqbal M, Abbas M, Nisar J (2019) Efficiency of immobilized Zea mays biomass for the adsorption of chromium from simulated media and tannery wastewater. J Mater Res Technol 8:75–86. https://doi.org/10.1016/j.jmrt.2017.05.016

Mohan D, Singh KP, Singh VK (2005) Removal of hexavalent chromium from aqueous solution using low-cost activated carbons derived from agricultural waste materials and activated carbon fabric cloth. Ind Eng Chem Res 44:1027–1042. https://doi.org/10.1021/ie0400898

Moradi F, Maleki V, Saleh-Ghadimi S, Kooshki F, Pourghassem Gargari B (2019) Potential roles of chromium on inflammatory biomarkers in diabetes: a systematic. Clin Exp Pharmacol Physiol 46:975–983. https://doi.org/10.1111/1440-1681.13144

Muxel AA, Gimenez SMN, De Souza Almeida FA, Da Silva Alfaya RV, Da Silva Alfaya AA (2011) Cotton Fiber/ZrO2, a new material for adsorption of Cr(VI) Ions in water. CLEAN - Soil, Air, Water 39:289–295. https://doi.org/10.1002/clen.201000165

Park SH, Shin SS, Park CH, Jeon S, Gwon J, Lee SY, Kim SJ, Kim HJ, Lee JH (2020) Poly(acryloyl hydrazide)-grafted cellulose nanocrystal adsorbents with an excellent Cr(VI) adsorption capacity. J Hazard Mater 394:122512. https://doi.org/10.1016/j.jhazmat.2020.122512

Peng X, Yan Z, Hu L, Zhang R, Liu S, Wang A, Yu X, Chen L (2020) Adsorption behavior of hexavalent chromium in aqueous solution by polyvinylimidazole modified cellulose. Int J Biol Macromol 155:1184–1193. https://doi.org/10.1016/j.ijbiomac.2019.11.086

Qiu B, Guo J, Zhang X, Sun D, Gu H, Wang Q, Wang H, Wang X, Zhang X, Weeks BL, Guo Z, Wei S (2014) Polyethylenimine facilitated ethyl cellulose for hexavalent chromium removal with a wide pH range. ACS Appl Mater Inter 6:19816–19824. https://doi.org/10.1021/am505170j

Rangabhashiyam S, Nakkeeran E, Anu N, Selvaraju N (2014) Biosorption potential of a novel powder, prepared from Ficus auriculata leaves, for sequestration of hexavalent chromium from aqueous solutions. Res Chem Intermed 41:8405–8424. https://doi.org/10.1007/s11164-014-1900-6

Rojas SI, Duarte DC, Mosquera SD, Salcedo F, Hinestroza JP, Husserl J (2018) Enhanced biosorption of Cr(VI) using cotton fibers coated with chitosan - role of ester bonds. Water Sci Technol 78:476–486. https://doi.org/10.2166/wst.2018.284

Sharma AK, Devan RS, Arora M, Kumar R, Ma Y-R, Babu JN (2018) Reductive-co-precipitated cellulose immobilized zerovalent iron nanoparticles in ionic liquid/water for Cr(VI) adsorption. Cellulose 25:5259–5275. https://doi.org/10.1007/s10570-018-1932-y

Shi X, Qiao Y, An X, Tian Y, Zhou H (2020) High-capacity adsorption of Cr(VI) by lignin-based composite: Characterization, performance and mechanism. Int J Biol Macromol 159:839–849. https://doi.org/10.1016/j.ijbiomac.2020.05.130

Simonin J-P (2016) On the comparison of pseudo-first order and pseudo-second order rate laws in the modeling of adsorption kinetics. Chem Eng J 300:254–263. https://doi.org/10.1016/j.cej.2016.04.079

Singh P, Chowdhuri DK (2017) Environmental presence of hexavalent but not trivalent chromium causes neurotoxicity in exposed drosophila melanogaster. Mol Neurobiol 54:3368–3387. https://doi.org/10.1007/s12035-016-9909-z

Song W, Gao B, Xu X, Xing L, Han S, Duan P, Song W, Jia R (2016) Adsorption-desorption behavior of magnetic amine/Fe3O4 functionalized biopolymer resin towards anionic dyes from wastewater. Bioresour Technol 210:123–130. https://doi.org/10.1016/j.biortech.2016.01.078

Sun Y, Liu X, Lv X, Wang T, Xue B (2021) Synthesis of novel lignosulfonate-modified graphene hydrogel for ultrahigh adsorption capacity of Cr(VI) from wastewater. J Clean Prod 295:126406. https://doi.org/10.1016/j.jclepro.2021.126406

Tariq MA, Nadeem M, Iqbal MM, Imran M, Siddique MH, Iqbal Z, Amjad M, Rizwan M, Ali S (2020) Effective sequestration of Cr (VI) from wastewater using nanocomposite of ZnO with cotton stalks biochar: modeling, kinetics, and reusability. Environ Sci Pollut Res Int 27:33821–33834. https://doi.org/10.1007/s11356-020-09481-x

Vakili M, Deng S, Li T, Wang W, Wang W, Yu G (2018) Novel crosslinked chitosan for enhanced adsorption of hexavalent chromium in acidic solution. Chem Eng J 347:782–790. https://doi.org/10.1016/j.cej.2018.04.181

Wang P, Yin Y, Xu J, Chen S, Wang H (2019) Facile synthesis of Cu2+-immobilized imprinted cotton for the selective adsorption of bovine hemoglobin. Cellulose 27:867–877. https://doi.org/10.1007/s10570-019-02816-z

Wei Y, Chen W, Liu C, Wang H (2021) Facial synthesis of adsorbent from hemicelluloses for Cr(VI) adsorption. Molecules 26:1443. https://doi.org/10.3390/molecules26051443

Wu Y, Zhang S, Guo X, Huang H (2008) Adsorption of chromium(III) on lignin. Bioresour Technol 99:7709–7715. https://doi.org/10.1016/j.biortech.2008.01.069

Xie B, Shan C, Xu Z, Li X, Zhang X, Chen J, Pan B (2017) One-step removal of Cr(VI) at alkaline pH by UV/sulfite process: reduction to Cr(III) and in situ Cr(III) precipitation. Chem Eng J 308:791–797. https://doi.org/10.1016/j.cej.2016.09.123

Xu X, Gao B, Jin B, Yue Q (2016) Removal of anionic pollutants from liquids by biomass materials: a review. J Mol Liq 215:565–595. https://doi.org/10.1016/j.molliq.2015.12.101

Yao F, Jia M, Yang Q, Luo K, Chen F, Zhong Y, He L, Pi Z, Hou K, Wang D, Li X (2020) Electrochemical Cr(VI) removal from aqueous media using titanium as anode: simultaneous indirect electrochemical reduction of Cr(VI) and in-situ precipitation of Cr(III). Chemosphere 260:127537. https://doi.org/10.1016/j.chemosphere.2020.127537

Zhang S, Chen H, Zhang S, Kai C, Jiang M, Wang Q, Zhou Z (2019) Polyethylenimine grafted H2O2-oxidized cellulose membrane as a novel biosorbent for Cr(VI) adsorption and detoxification from aqueous solution. Cellulose 26:3437–3453. https://doi.org/10.1007/s10570-019-02325-z

Zhao J, Boada R, Cibin G, Palet C (2021) Enhancement of selective adsorption of Cr species via modification of pine

biomass. Sci Total Environ 756:143816. https://doi.org/10.1016/j.scitotenv.2020.143816

Zhao J, Zhang X, He X, Xiao M, Zhang W, Lu C (2015) A super biosorbent from dendrimer poly(amidoamine)-grafted cellulose nanofibril aerogels for effective removal of Cr(vi). J Mater Chem A 3:14703–14711. https://doi.org/10.1039/c5ta03089g

Zheng C, Zheng H, Sun Y, Xu B, Wang Y, Zheng X, Wang Y (2019) Simultaneous adsorption and reduction of hexavalent chromium on the poly(4-vinyl pyridine) decorated magnetic chitosan biopolymer in aqueous solution. Bioresour Technol 293:122038. https://doi.org/10.1016/j.biortech.2019.122038